A PIV/PTV system for analysing turbulent bubbly flows

D. Bröder and M. Sommerfeld

Institut für Verfahrenstechnik / Mechanische Verfahrenstechnik
Fachbereich Ingenieurwissenschaften
Martin-Luther-Universität Halle-Wittenberg
D-06099 Halle (Saale), Germany
Email: martin.sommerfeld@iw.uni-halle.de

ABSTRACT

Bubble columns are widely used in chemical industry and biotechnology. Flow and turbulence in such an apparatus are induced by the bubble rise, and the bubble behaviour is strongly affected by swarm effects (i.e. the interaction between bubbles). For analysing the bubble swarm behaviour and simultaneously evaluating the flow structure and bubble-induced turbulence in a bubble column of 140 mm diameter and a height of 650 mm (initial water level) Particle Image Velocimetry (PIV) was applied. The bubble column was aerated with relatively fine bubbles with a size distribution between about 0.3 and 4.0 mm. The gas hold-up was varied in the range between 0.5 and 4 %.

A two-phase PIV-system was developed to evaluate instantaneous flow fields of both rising bubbles and the continuous phase (Fig. 1). The measurement of the liquid velocities in the bubble swarm was done by adding fluorescing seed particles. Images of bubbles and fluorescing tracer particles were acquired by two CCD cameras. The signals from tracers and bubbles were separated by optical interference filters with a band width corresponding to the emitting wavelength of the fluorescing tracer particles and the wavelengths of the applied Nd-YAG pulsed laser. To improve the phase separation of the system the CCD cameras were placed in a non-perpendicular arrangement with respect to the light sheet.

The acquired images were evaluated with a cross-correlation algorithm developed by Gui et al. (1997). In order to obtain information about bubble motion and the local velocity of the fluid 500 to 1000 image pairs were recorded and evaluated. By averaging the instantaneous velocities of bubbles and fluid, mean velocities and fluctuating components could be obtained. In addition turbulence intensities were deduced from the measurements. The turbulence properties were used to characterise bubble-induced turbulence for various bubble mean diameters and gas hold-ups. Moreover, the determination of the average bubble slip velocity within the bubble swarm was possible.

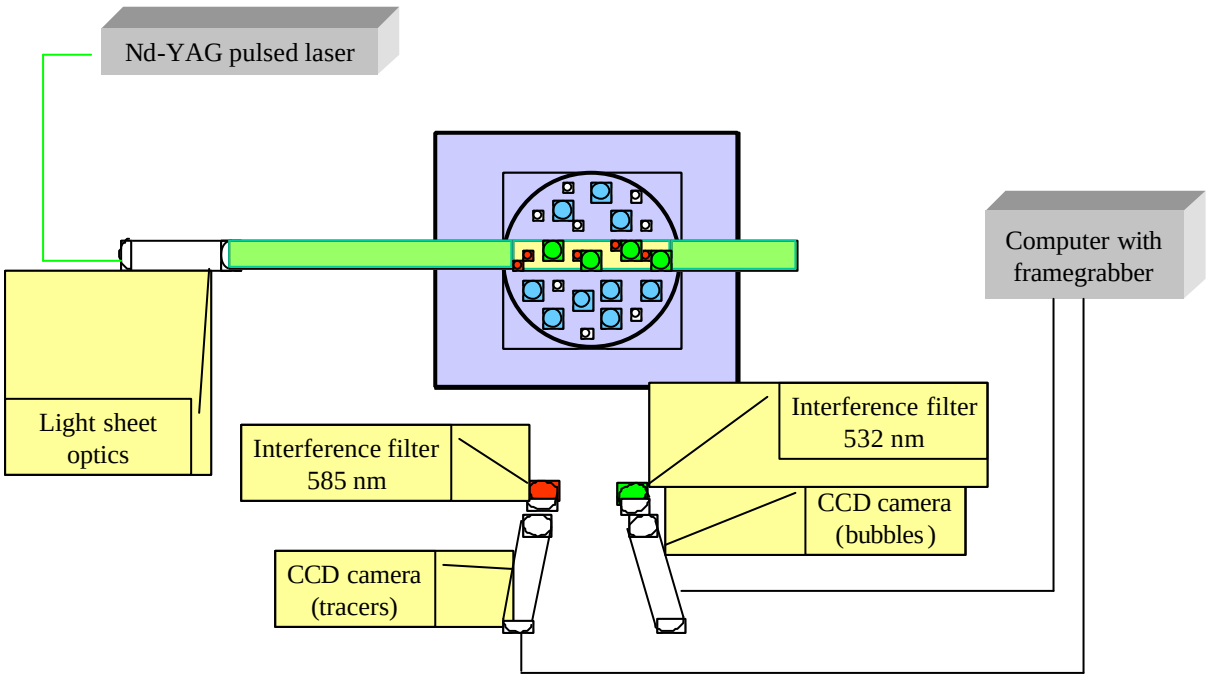

Figure 1: Two-phase PIV-system

1. INTRODUCTION

In order to analyse bubbly flows several measurement techniques have been developed and applied during the last years. Taking no notice of integral methods, mainly used to determine the void fraction, phase-Doppler and laser-Doppler velocimetry, acoustic measurement techniques, particle image velocimetry, particle tracking velocimetry, and holographic techniques should be mentioned. Many of these analysing methods do register only the properties of one phase. A combination of more than one method is necessary to characterise the properties of both phases. Simultaneous measurements of both phases are rarely possible and limited to simple experimental arrangements. Many highly developed techniques like phase- and laser-Doppler velocimetry provide highly precise information of bubble sizes and velocities of bubbles and liquid. But low data rates caused by low bubble number concentrations and velocities and light absorption give rise to very long sampling times per measurement point. This means that the measurement of a complete flow map in an apparatus, which is necessary for comparisons with numerical simulations, is hardly possible because of long measurement periods. Additionally phase-Doppler velocimetry is limited by the bubble size in its application. Because of their non-spherical shape, bubbles with more than about 1 mm diameter can not be sized correctly with PDA (Tassin & Nikitopoulos 1995). For a 1 mm ellipsoidal bubble in water the ratio between the length of the main axses is 1.15 (Duineveld 1994). This means consistency errors in determining the phase differences of Doppler bursts and hence considerable errors in determining the size of these bubbles. Modern camera optical measurement techniques like PIV are able to realise complete planes of a flow and together with methods of digital image processing techniques it is possible to provide velocities, sizes and also information about shape and position of bubbles.

2. TEST FACILITY

The bubble column used in the present investigations has a diameter of 140 mm and a height of 650 mm (i.e. water level in the column). In order to reduce refraction effects at the curved wall, the bubble column is placed in a square vessel which also is filled with tap water. The aerator is build using a porous membrane with a pore size of 0.7 µm. In order to fix the membrane it is mounted between two perforated plates, which are screwed on top of a small stagnation chamber. The aerator is connected via a flow meter to a pressurised air supply system. Once the aerator is pressurised the membrane bulges and small bubbles are produced at the holes of the perforated plate so that a homogeneous aeration is established over the cross-section of the aerator with a diameter of 100 mm. The gas flow rate was varied by increasing the supply pressure. As a result of the stronger bulging of the membrane at higher pressures also the bubble size was increased with gas flow rate. Hence measurements were performed for different gas hold-up up to about 4 % and different bubble size spectra in the range between 0.3 and 4 mm. In order to reduce bubble coalescence propanol was added to the tap water at a volume concentration of 0.004 %.

3. TWO-PHASE PIV SYSTEM

The application of PDA for analysing bubbly flows with bubbles of diameters larger than 1mm is not recommended because of the non-spherical shape of these bubbles (Fig. 2) and low data rates of the sampling process. Hence a two-phase PIV system for simultaneous measurements of the velocities of both phases was established. The measurement of the liquid velocities in the bubble swarm was done by adding fluorescing seed particles of a mean diameter of 50 µm. The maximum in the absorption spectrum of these tracers is about 530 nm and so it is close to the wavelength of the applied pulsed Nd-YAG laser (532 nm). An optical interference filter corresponding to the emitting wavelength of the fluorescing tracer particles mounted on the optics of a CCD camera (Sony XC 75) provided images of the tracers without reflections from the bubbles. Hence with this images a phase separated determination of the liquid velocities was possible. Images of the bubbles were recorded by a second CCD camera. This camera was fitted with an optical interference filter corresponding to the wavelength of the applied laser. Images of bubbles recorded by this camera showed bubbles only as points because of reflections on the surface of bubbles. It was not possible to realise the contours of bubbles or tracers because of their low scattering light intensity.

Multiphase flows take high demands to optical measurement techniques because of often difficult optical access. In case of PIV the main problems are caused by large optical path lengths in the flow and high void fractions. Also the mean bubble size is important because for low void fractions but small bubbles the number concentration of bubbles is high and apparatus volume becomes opaque. In order to get information from the core of a bubbly flow it is necessary to minimise disturbances caused by light scattering of bubbles outside the plane illuminated by the light sheet.

PIV recordings except for Stereo-PIV are typically done in a perpendicular arrangement of the camera with respect to the light sheet. It turned out that this perpendicular arrangement was not suitable for taking images of bubbles in a light sheet because the scattering light intensity of air bubbles in water decrease strongly for off-axis

angles larger than φ_c=82,5° (Fig.3). This implies that for a perpendicular arrangement of the camera with respect to the light sheet, a low contrast between bubbles inside and outside the light sheet plane. In order to enhance the contrast for bubbles inside the light sheet the CCD camera was placed at an off-axis angle of about 80° with respect to the plane of the light sheet. Off-axis angles in this range have been also recommended for PDA measurements (Tassin & Nikitopoulos 1995, Crowe et al. 1998, Sommerfeld & Bröder 1999).

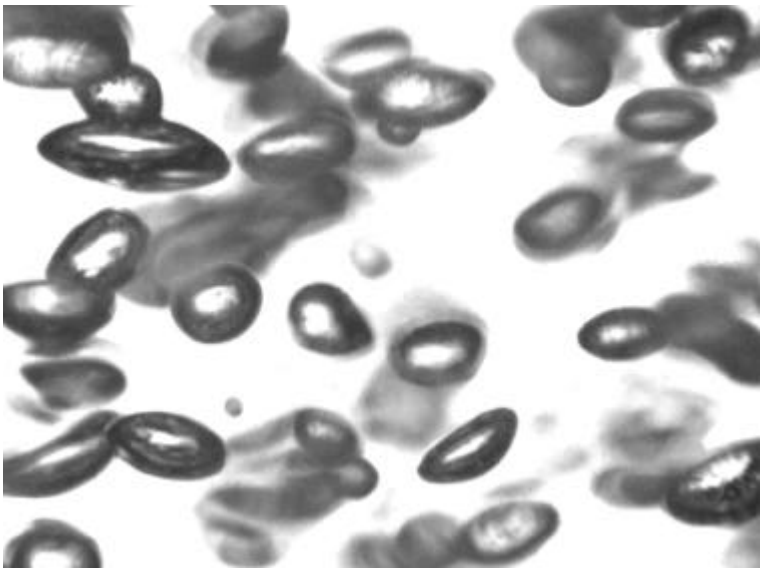

Figure 2. Typical image of bubbles in the core of the bubble column. The image was made by back lightning the scene with a pulsed LED-array. The focal length was 108 mm, and the aperture was completely open to provide a short depth of focus. The gas hold-up was 2,92%,and the mean bubble diameter was 3 mm.

The CCD camera for recording images of the fluorescing tracer particles was placed at an off-axis angle of 105° close to the angle of Brewster conditions for first order reflection of φ_B=106,1° for a system with a relative refractive index of 0.75 (Fig. 3). At the Brewster angle reflection of light polarised parallel to the plane of the light sheet is extinguished. Hence around this off-axis angle a minimum of the scattering intensity from bubbles inside the light sheet is observed (Fig. 4). The additional application of the described interference filter for the emitting wave length of the fluorescing tracers provided an excellent phase separation for the recorded images.
The applied camera optics were zoom lenses with a variable focal length of 18 ÷ 108 mm. The aperture and focal length of the optics were adjusted in such a way to provide sharp images over the whole range of the observation area. Distortions within the recorded images caused by the non-perpendicular arrangement of both cameras were corrected by a geometric transformation based on the perspective projection.

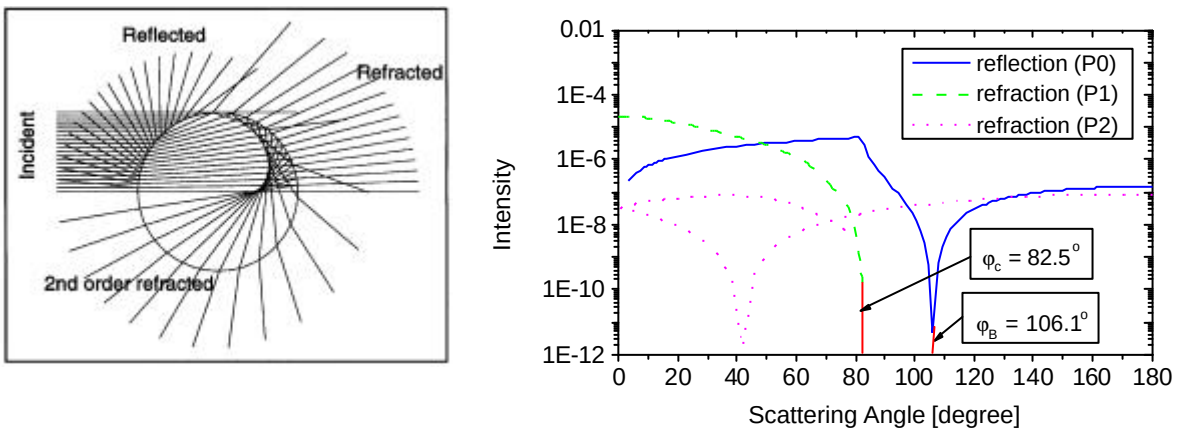

Figure 3: Air bubble in water. Left panel: ray tracings; Right panel: angular dependence of relative intensity for the different scattering components (logarithmic scale) for parallel polarisation.

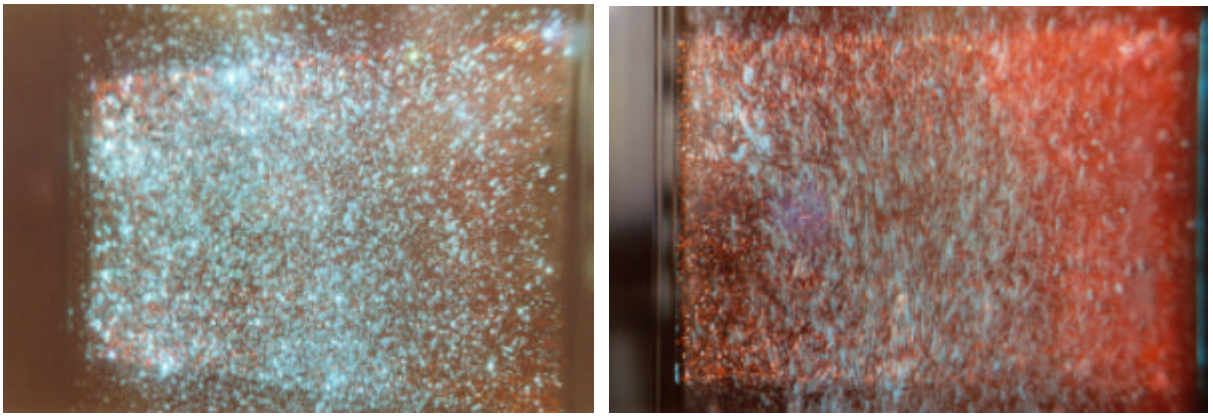

Figure 4: Pictures of the laser light sheet with bubbles and fluorescing tracer particles recorded by colour photography. The applied laser was a continuous wave argon ion laser. The pictures show the influence of the arrangement of the camera with respect to the light sheet. The left picture was taken at an off-axis angle of about 80°, here the light intensity of bubbles in the light sheet is high. The right picture was taken at a off-axis angle of about 105°, the bubbles in the light sheet are nearly invisible and only some bubbles outside the light sheet can be seen.

The light sheet optics and both CCD cameras were mounted on a computer controlled traverse-system to perform automatic measurements in different heights of the bubble column. The images of both cameras were acquired by two framegrabber cards mounted in a PC, compressed and stored on the harddisk of the PC for some later evaluation. The compression of the images was performed by the JPEG-technique (Joint Photographic Experts Group) with compression ratios up to 1:10 to reduce the memory capacity of one measurement from 6.2 GB to the capacity of a writeable compact disc (CD-R). The JPEG-technique applied in PIV for determining mean and fluctuating fluid velocities has been described by Freek et al. (1999). Additional evaluation uncertainties caused by the compression were determined to be smaller than 0.1 pixel and are therefore in the same range like the accuracy of the evaluation method. The evaluation of the recorded images is performed by an in-house developed software based on the Minimum-Quadratic-Difference (MQD) method of Gui et a. (1997).

In order to enhance the image quality which is influenced by the difficult optical access some operations of digital image processing are necessary before the cross-correlation was performed by the MQD-algorithm. Within this steps the image background which is caused by bubbles outside the light sheet was removed by a unsharp-mask filter and the image contrast was enhanced.

The cross-correlation was performed in an iterative multigrid approach with a successive refinement of the size of the interrogation areas (Fig. 5). With this approach described by Scarano & Riethmuller (1999) it was possible to provide a high local resolution without influencing the accuracy of the evaluation because of small interrogation areas. In a first step a raw displacement-map was evaluated with a interrogation area size of 50*50 up to 60*60 pixel. This displacement-map was used as a predictor for a next cross-correlation with a interrogation area size of 50 % of the interrogation area size of the first cross-correlation. The vectors of the displacement-maps of each cross-correlation were checked for criteria of SNR ratio and only validated vectors were used as predictor information. In following iteration steps the cross-correlation was performed only for small displacements around the predictor, so the evaluation of this iteration steps is accelerated. The displacement-map of the second cross-correlation was used as a predictor for a last cross-correlation with a interrogation area size of 15*15 pixel. The local resolution of the image for the bubbles is 0.1882 mm/Pixel in the horizontal and 0.3598 mm/Pixel in the vertical direction. For the images of tracers the local resolution is 0.1288 mm/Pixel horizontal and 0.2477 mm/Pixel vertical. Therefore, the local resolution of the last cross-correlation amounts to 1.9*3,7 mm for the tracers and 2.8*5.4 mm for the bubbles. The mean bubble distance L for a cubic arrangement is 5.89 mm for a mean bubble diameter D_B of 2.5 mm and a void fraction α of 4 % and hence is larger than the local resolution of the cross-correlation.

$$L = D_B\left(\frac{p}{6a}\right)^{1/3} \tag{1}$$

Therefore, within the first iteration steps groups of bubbles inside an interrogation area were evaluated but in the last cross-correlation in average the displacement of only single bubbles was determined. Hence, the velocity evaluation technique changes from PIV to PTV for the bubbles.

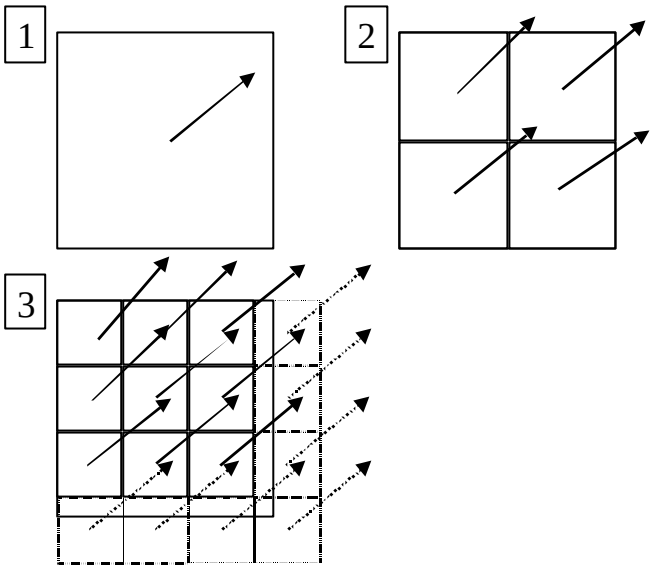

*Figure 5. Scheme of the successive refinement of the interrogation area size. The size of the interrogation areas amount to 50*50, 25*25 and 15*15 pixel, respectively (small structures of a flow like vortices were resolved only by small interrogation area sizes).*

Earlier investigation of the bubble column performed by LDA with a seeding of fluorescing tracer particles to analyse liquid velocities have shown that the flow inside the column was characterised by low frequency fluctuations. These fluctuations were caused by non-periodic tumble movements of the rising bubble plume in the lowest section of the bubble column and it was possible to measure their influence also in the highest section of the column. Fig. 6 shows the time series of the axial component of the liquid velocity of such a LDA measurement. The cumulative mean velocity has even after a measurement period of 600 s still not reached a final value. Therefore, the measurement periods for flow measurements in the bubble column shall be performed for more than 10 min to provide reliable averaged results.

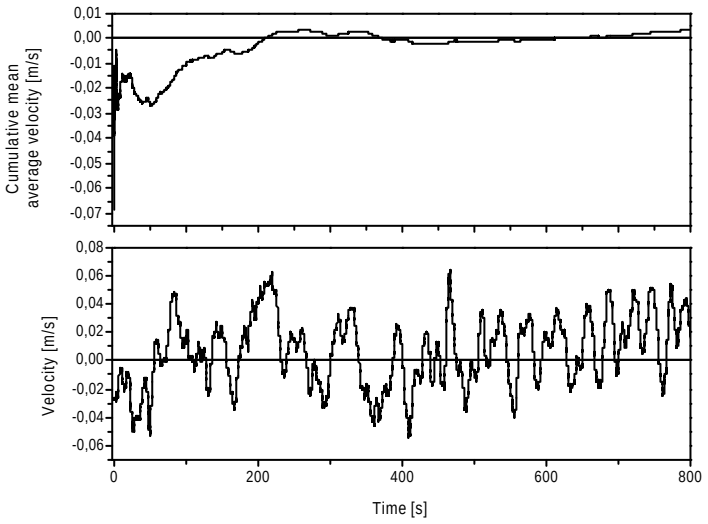

Figure 6. Time series of the axial liquid velocity measured with LDA and fluorescing tracer particles. The position of the measurement was 450 mm above the membrane aerator and the radial position was 50 mm. The mean flow velocity was 0.0035 m/s and the fluctuating velocity was 0.059 m/s. The upper graph shows the

course of the cumulative mean velocity, the lower graph shows the smoothed course of the instantaneous velocity.

In order to provide averaged velocity information of both phases by means of PIV, 1000 ÷ 2000 images per phase and section were recorded during a period of about 20 min. This resulted in an averaging of 500 ÷ 1000 validated vector-maps per phase. The difficult optical access and environment was the reason for missing vectors in the vector-maps since these vectors were not validated. Especially parts of the images with large optical path length of the light sheet were concerned because the light intensity was reduced by absorption and light scattering on bubbles (Fig. 7). This reduction of light intensity was realised especially for images of the fluorescing tracer particles. Therefore, the width of the images of tracers was usually 80 mm, while images for the bubbles were recorded over the complete cross-section of 140 mm.

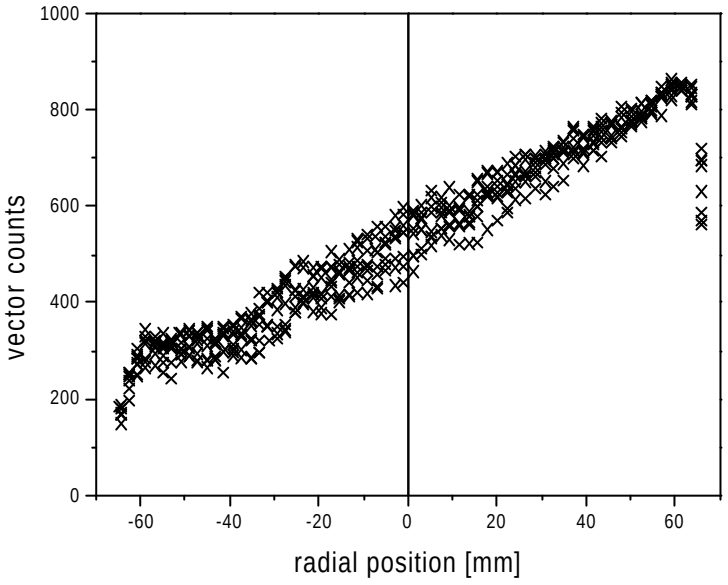

Figure 7. Influence of the optical path length of the laser light sheet on the number of validated vectors. (Cumulating of over 1000 vector-maps of bubble velocity in one section.)

4. RESULTS

The main reason to develop and apply the described measurement technique was to provide reliable detailed data for the validation of numerical simulations. Comparisons between numerical flow predictions and results of investigations by flow measurement shall provide qualitative and quantitative statements about discrepancies and agreements between simulation and "measured" reality. Results of investigations by PIV fill this demands like no other technique. The result of the evaluation of a single double frame provides information about the appearance of occurring flow structures like the techniques of flow visualisation do (Fig. 8). In addition a vector-map contains precise velocity information for a large number of points or areas to allow quantitative comparisons.

By averaging a large number of vector-maps it is possible to calculate mean and fluctuating velocities and also turbulence parameters. A few examples of determinated flow parameter are given in the following. It is worth to mention that there exist more possibilities to determine characteristic parameters, such as correlations between the phase properties. A detailed investigation of the hydrodynamic interactions between both phases will lead to a sophisticated modelling of bubbly flows.

A few results of a investigation of the bubble column are shown in Fig. 9. There are shown the vector-maps of the averaged bubble U_{Bub} and liquid velocities U_{Liq} and slip velocity U_{Slip} calculated by:

$$\overline{U}_{Slip} = \overline{U}_{Bub} - \overline{U}_{Liq} \tag{2}$$

The turbulent kinetic energy of the fluid k was calculated by:

$$k = \frac{1}{2}\left(\overline{u'^2} + 2\overline{v'^2}\right) \tag{3}$$

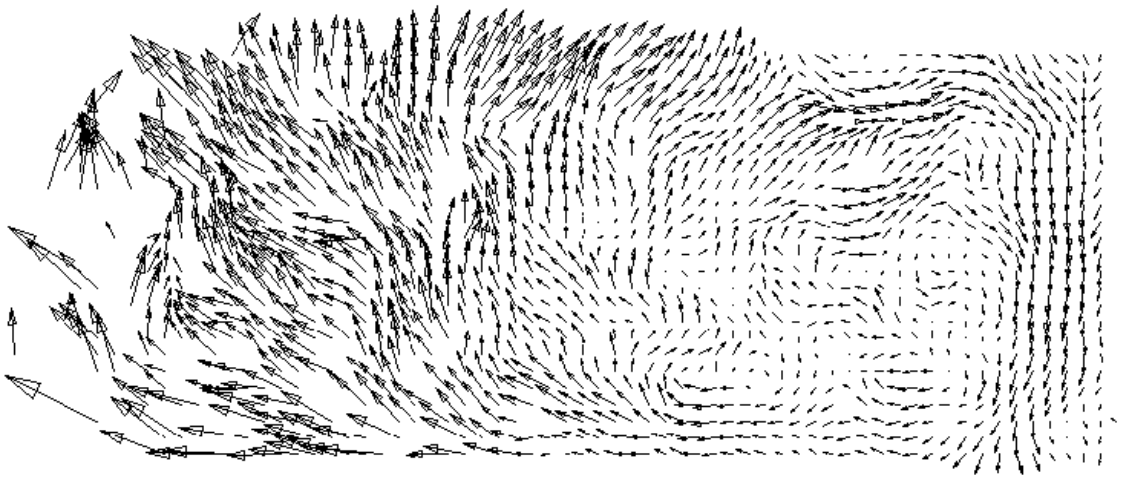

Figure 8. Instantaneous flow field of the continuous phase in the bubble column. Left side is close to the core, the right side is close to the wall. Missing vectors at the left side are caused by low scattering light intensity of the fluorescing tracer particles.

The superficial gas velocity for this experiment was 0.3 cm/s. The mean gas hold-up was 1.7 % and the mean bubble diameter was about 2 mm. The velocities of the rising bubbles reach the highest values close to the vertical axis of the column and its lowest values close to the wall within a height of about 100 mm above the aerator. The reason for some missing vectors close to the wall for heights smaller than 50 mm was the low local void fraction in this area. The applied membrane aerator had a smaller diameter than the inner diameter of the bubble column. Therefore, the rising bubble plume dispersed from that diameter and was contacted by the liquid coming down near the wall. Due to the rising bubble plume in the core of the column the liquid is pushed upward and moves downward close to the wall. The flow field is not symmetric with respect to the vertical axis of the column which is caused by some small inhomogeneity of the membrane aerator. The areas of the highest upward (h=250, r=0) and downward (h=80, r=65) liquid velocities agree with the areas of highest and lowest velocities of the rising bubbles. The slip velocity calculated from the mean velocity fields of bubbles and liquid shows some decay to the wall for the lowest section of the column caused by the higher local void fraction in the core.

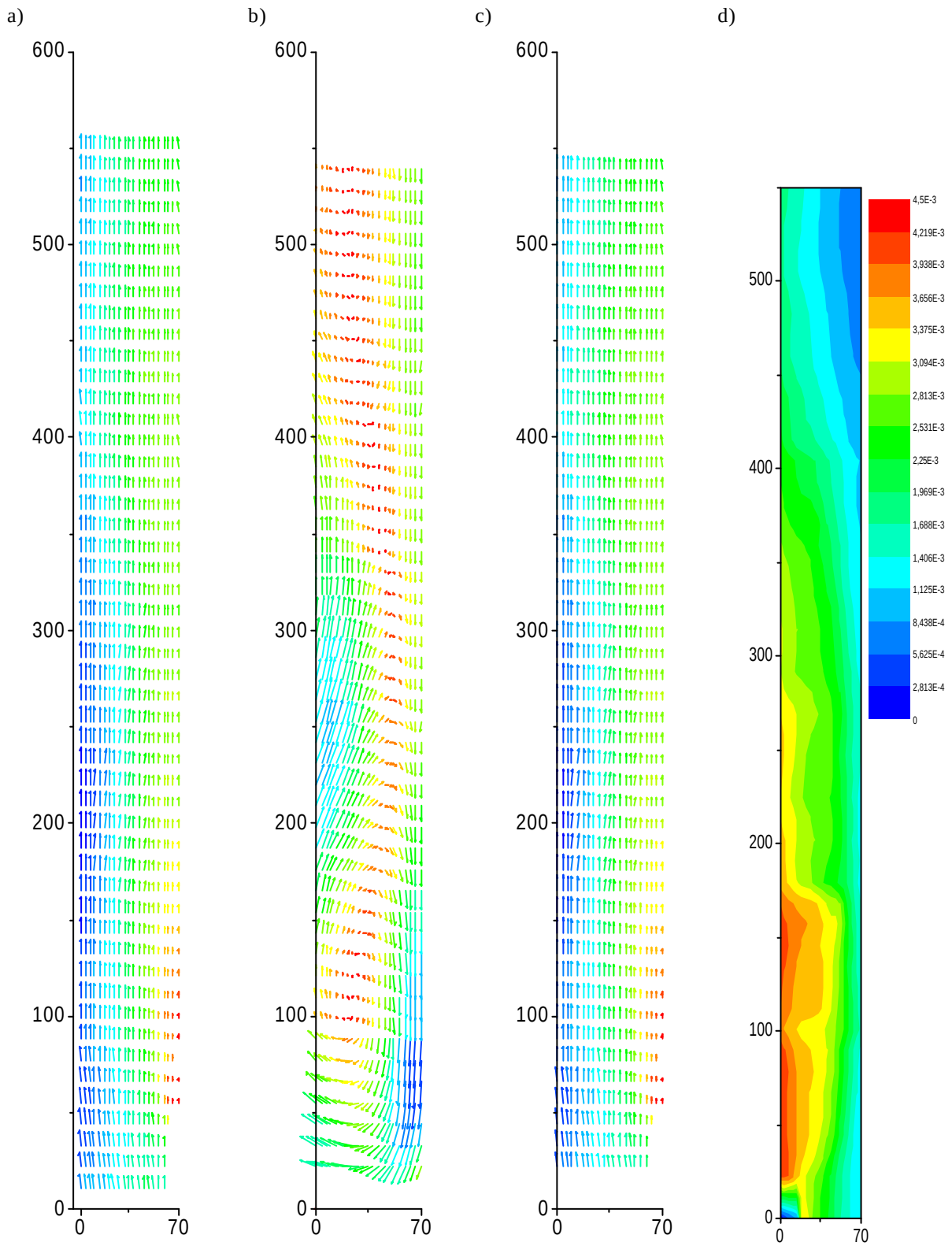

Figure 9. From left to right: vector plots of the averaged velocity fields of bubbles (a), liquid (b) and slip velocity (c); contour plot of the turbulent kinetic energy of the fluid (d). (The different vector plots do not have the same scaling.) The superficial gas velocity was 0.3 cm/s, the mean gas hold-up was 1,7 %, and the mean bubble diameter was 2 mm.

With increasing height the bubbles were dispersed homogeneously and in the top section the slip velocity is nearly constant over the complete cross-section. The turbulent kinetic energy of the continuous phase shows a

maximum for the areas of the highest local void fraction and high bubble dispersion in the core region next to the aerator. In the course of the flow the turbulent kinetic energy decreased to half of the maximum value. The described phenomena are shown more clearly in Fig. 10 and Fig. 11 than in the qualitative account of Fig. 9. Here velocities of bubbles, liquid and slip velocity are shown here as profiles for two cross-sections in different heights of the bubble column. The profile of the slip velocity for a height of 120 mm shows clearly a constant slip velocity for the core and a decay for the regions of low local void fractions close to the wall. The profiles for a height of 480 mm are in general flatter than the profiles of the lower region and the slip velocity is nearly constant over the entire cross-section. The axial and radial components of the fluctuating velocities for both phases are shown in Fig. 11. Also here the profiles for the height of 480 mm are flatter than for the height of 120 mm. The fluctuating velocities of the bubbles for both heights are of the same order, and the fluctuating velocities of the fluid are smaller for the upper profiles. The difference between the axial and radial component of the profiles of the liquid shows the anisotropic turbulence character of the bubbly flow.

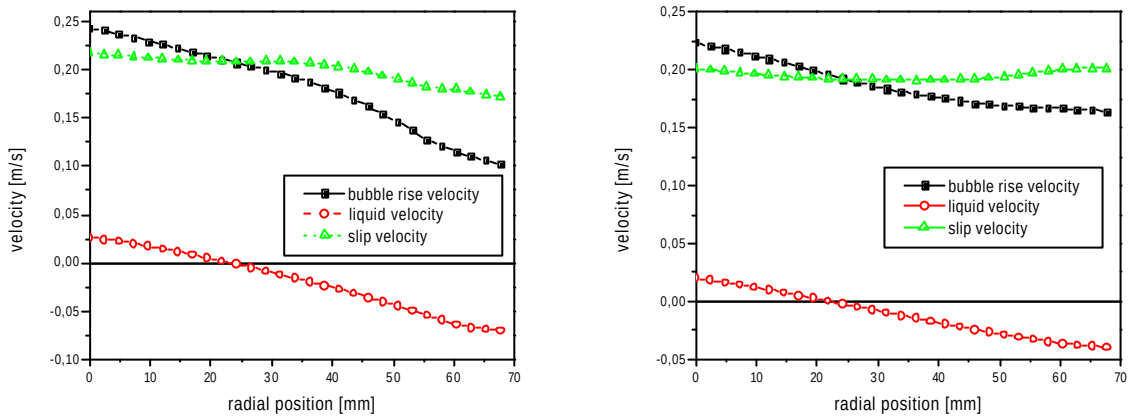

Figure 10. Profiles for the velocities of bubbles, liquid and slip velocity for different heights in the bubble column. Left: height=120 mm; Right: height=480 mm.

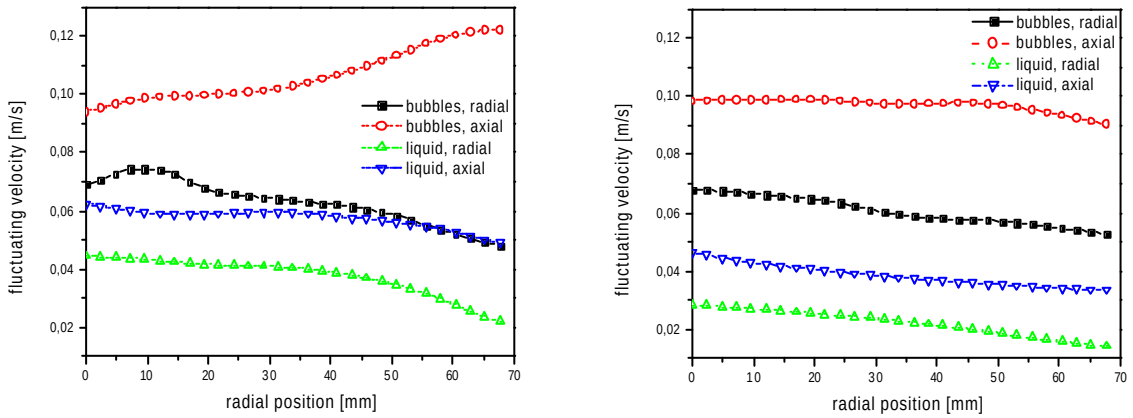

Figure 11. Profiles for the fluctuating velocities of bubbles and liquid for different heights in the bubble column. Left: height=120 mm; Right: height=480 mm.

Conclusion

A measurement system for simultaneous determination of the velocities of both phases in a bubbly flow has been developed. The technique works on the principle of PIV with an iterative refinement of the interrogation area size. The evaluation and the statistical averaging of a large number of PIV recordings provides mean and fluctuating flow velocities. The measurement system was tested and applied to a bubble column to provide data for validation of numerical simulations. In future works the post-processing will be enhanced to allow sophisticated investigations of hydrodynamic interactions.

ACKNOWLEDGEMENTS

The financial support of the present studies by the Deutsche Forschungsgemeinschaft under contract number SO 204/13 is gratefully acknowledged.

REFERENCES

Clift, R., Grace, J., & Weber, M. E. 1978. Bubbles, drops and particles. New York:Academic Press

Crowe, C.T., Sommerfeld, M. & Tsuji, Y. 1998, Multiphase Flows with Droplets and Particles. CRC Press, New York.

Freeek, C., Sousa, J.M.M., Hentschel,W., Merzkirch, W. 1999, On the accuracy of a MJPEG-based digital image compression PIV-system, Experiments in Fluids, Vol 27, 310-320.

Gui, L.; Lindken, R.;Merzkirch, W. 1997, Phase-separated PIV Measurements of the Flow Around systems of Bubbles Rising in Water; ASME-FEDSM97-3103

Lain, S., Bröder, D., Sommerfeld, M. 1999 Experimental and numerical studies of the hydrodynamics in a bubble column. Chemical Engineering Science, 54, 4913-4920

Scarano, F., Riethmuller, M.L. 1999, Iterative multigrid approach in PIV Image processing with discrete window offset, Vol.26,513-523.

Sommerfeld, M., Bröder, D. 1999, Untersuchung der Hydrodynamik einer Blasensäule mittels der Phasen-Doppler-Anemometrie. In: Lasermethoden in der Strömungsmeßtechnik (Eds. Pfeifer et al.) Shaker Verlag, Paper 35.1-6.

Tassin, A.L. & Nikitopoulos, D.E. 1995, Non-intrusive measurements of bubble size and velocity. Experiments in Fluids, Vol. 19, 121-132.